The 40m RT IF spectral behaviour at 5, 22 and 87 GHz

P. de Vicente

Informe Técnico IT-OAN 2012-03

Revision history

Version	Date	Author	Updates
1.0	16-12-2011	P. de Vicente	First version

Contents

1 Introduction

We have investigated the IF spectrum from the C band, 22 GHz and 87 GHz receivers after the installation of new preprocessors in front of the FFT backend, and summarize the resuls below. We conclude that the band should be equalized and tests should be repeated after, to test its benefit. We also show that the most important problems can be avoided using a software solution that calibrates the observations per frequency channel.

2 The problem

Fig. 1 shows the LCP spectrum towards source CB3 at 24 GHz. The integration time was 272 minutes and the average system temperature 80 K. The spectrum was obtained averaging 544 on-off scans of 30 seconds integration time per subscan. The spectral line at 23870 GHz is NH_3 3(3)-3(3). This spectrum is a typical sample of those obtained with the Yebes 22 GHz receiver up to now: the noise increases from high to low frequencies, there is a relative noise minimum at 23930 GHz (180 MHz in the IF band) and the baseline shows non uniform ripples. These lack of flatness, ripple behaviour and apparent different noise along the band is a serious problem which prevents observations of large width spectral lines, like those from galaxies, or emission with wings from outflows. It is also a problem for comparing spectral lines which are simultaneously detected along the band.

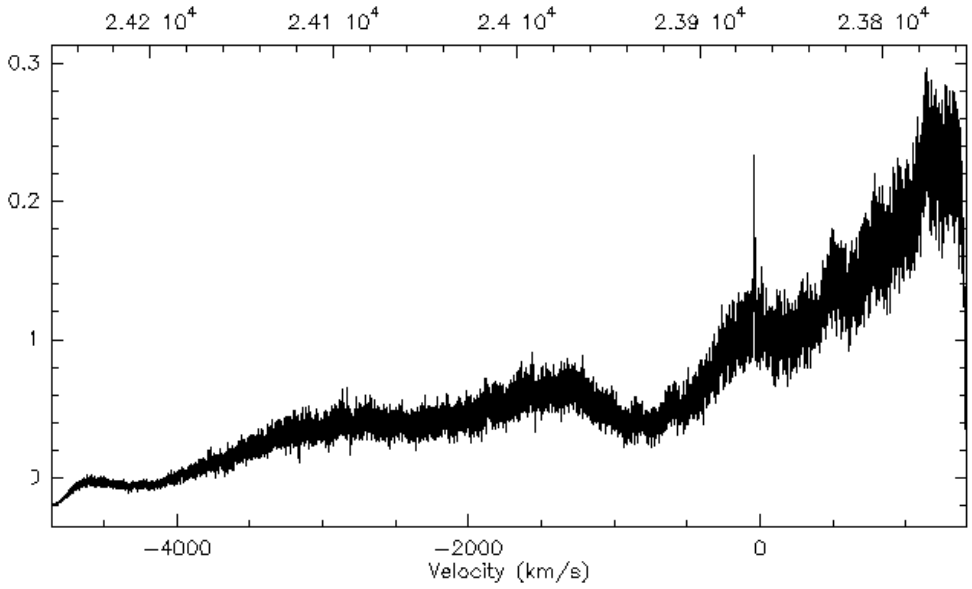

Figure 1: *Spectrum towards CB3 at 24 GHz. Integration time was 272 minutes. The spectrum was obtained averaging several on-off scans 30 seconds integration time long. This spectrum exemplifies the problems exposed in this report: lack of flatness, ripples and variability of the signal to noise ratio along the band.*

In the next sections we investigate the problem further to determine the causes and possible solutions.

3 The IF spectrum

The IF from the C band, 22 GHz and 3 mm receivers goes from 500 to 1000 MHz to match the input bandwidth of the VLBA terminal. Currently the signals are patched manually in the receiver cabin and in the backends room. The cables, an XXXX model, for both polarizations are shared by the 3 receivers. Whenever an observation is performed the IF signals are connected to IFs A and C of the VLBA terminal. The signals are then recovered in the Output Monitor connectors of the VLBA IF modules and injected into inputs 3 and 4 of the FFT. Each of these two inputs are connected to two modules respectively programmed to deliver 500 MHz bandwidth spectra with a resolution of 16384 channels.

When the detected signal is weak or there is no detectable signal, the FFT does not display a clean and flat baseline. The aspect varies as a function of the receiver. See panels in Fig. 2 which contain spectra at 5 GHz, 23 GHz and 87 GHz. These spectra were obtained from an on-off scan with an integration time of 30 seconds on each phase towards several galactic sources.

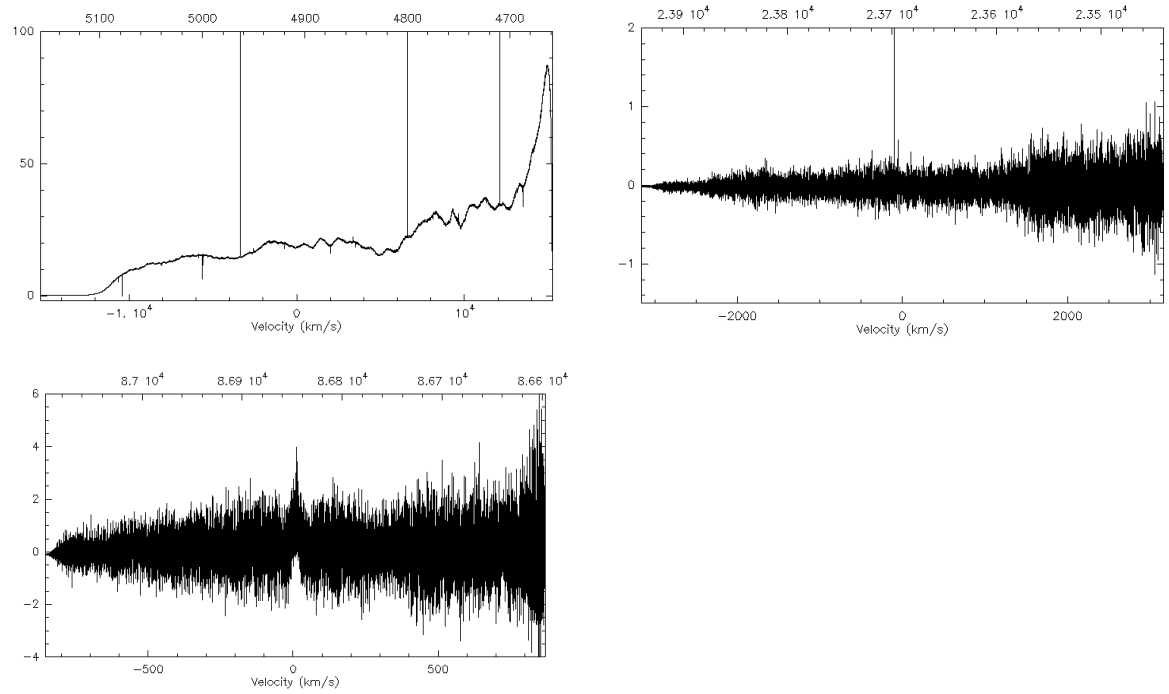

Figure 2: *Spectra for the C band (upper left), 22 GHz (upper right) and 87 GHz (lower left) receivers after an on-off scan of 30 seconds integration time in each phase towards several galactic sources.*

The C band receiver spectrum shows that the on-off scan does not remove the slope of the band. The band shows many variations, including interferences along the band that render it almost useseless.

The 22 GHz and 87 GHz receiver spectrum show a common behaviour. The baseline is roughly flat but the RMS noise is not uniform along the band: there is a minimum at the highest 20 MHz in the band, and a maximum at the lowest frequencies. The minimum is caused by the response of the passband filters.

Integration of many 30 seconds on-off scans may result in spectra with worse baselines. Fig. 3 shows two on-off scans at 23 GHz: one with 30 seconds integration time and superposed on it (red line), one with 140 minutes integration time. The lack of flatness and ripples in the long integration on-off scan are not visible in the short integration time on-off scan due to the higher noise.

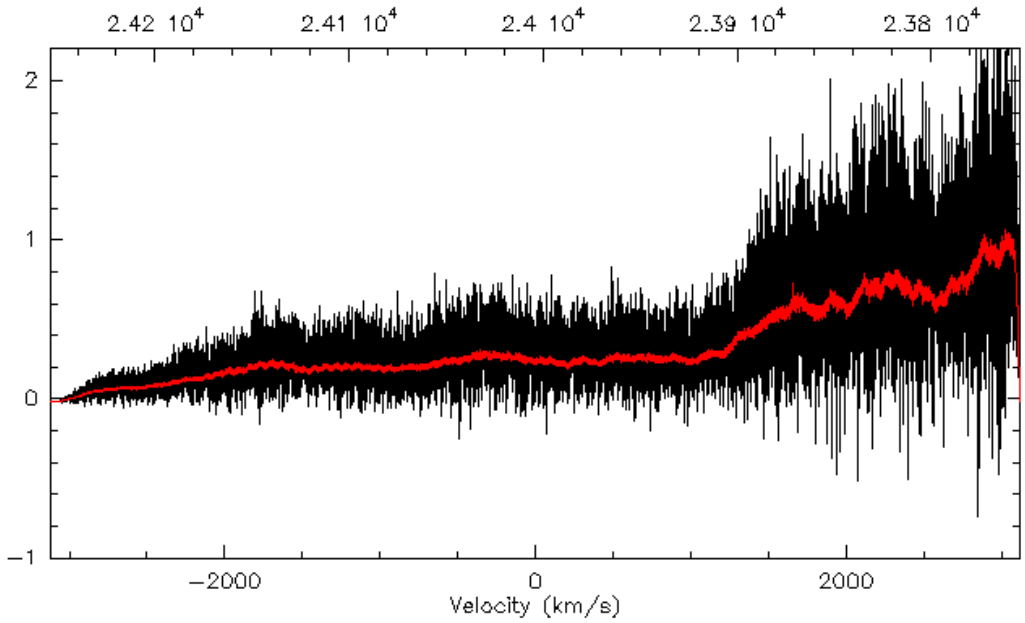

Figure 3: *Black line: spectrum at 23 GHz towards I2272+6858 after 30 seconds integration, red line: spectrum after 140 minutes integration. The spectra were obtained with an spatial on-off scan*

The noise difference along the band is probably associated to the difference of input power along the band.

Fig. 4 displays the input power in dBs along the band. The power drops more than 10 dB in 500 MHz for the C band and 22 GHz receivers. The power drop for the 87 GHz is slightly less than in the other cases. The band shows ripples of different frequencies which usually disappear after an ON-OFF scan. Inspection of Fig. 4 shows that the curves have a very similar behaviour for the 3 receivers: a steep slope in the first 50 MHz, a plateau with ripples between 50 and 100 MHz, a small upwards slope and then a new decrease of power at 160 MHz, up again at 210 MHz, down at 250 MHz, up at 2670 MHz and then a long bow whose power decreases with frequency. The decrease is stronger at C band and smaller at 87 GHz. The slope along the IF band shared by the three receivers points towards the cables as the most probable cause for such behaviour.

In order to check if the band behaviour is related to the power drop along the band we show

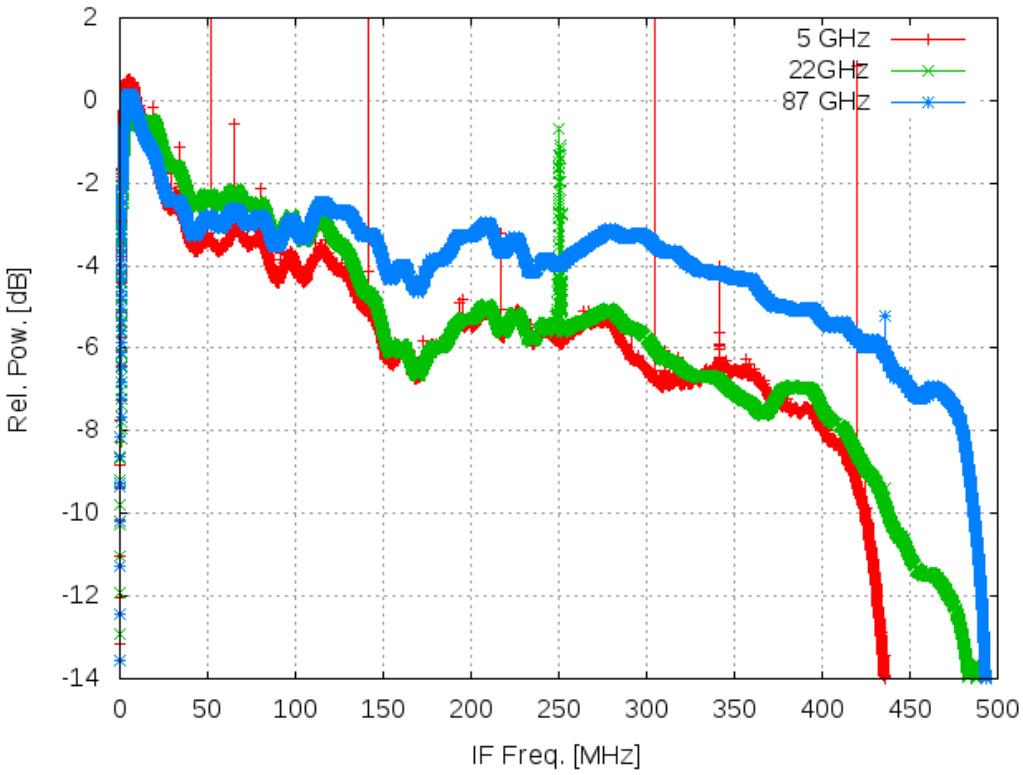

Figure 4: *Input power in the FFT at C band, 23 GHz and 87 GHz*

the spectrum, and the ON and OFF spectra for the 23 GHz receiver simultaneously in Fig. 5a. The ON and OFF subscans are in dBs while the scale of the ON subscan minus the OFF subscan is in arbitrary linear units. According to the figure, an increase of the noise along the band is associated to the input power: the highest the power, the highest the peak to peak noise. In order to check this hypothesis we have plotted in Fig. 5b the ON minus OFF power versus the input power. The envelope of the data is a straight line, such that a reduction of approximately 2.7 dB of power decreases the peak to peak noise by 2.

The previous figure also shows that, within the scale displayed in the figure, the ON and OFF subscans cannot be distinguished.

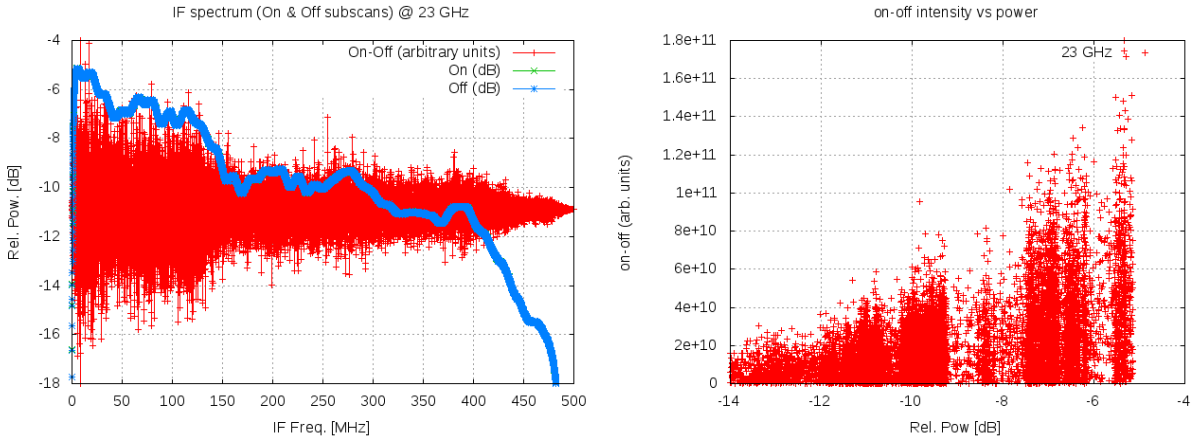

Figure 5: *Left: a) IF spectrum at 23 GHz. We have superposed the on and off subscans in dB (they cannot be distinguished). on-off in arbitray units (no log scale). Right: b) on-off in arbitrary units versus on power in dB. The envelope of the graph shows that there is a linear relation between the input power and the peak to peak noise of the on-off spectrum*

The main conclusion is that an equalizer should be installed to minimize this effect. Tests after the equalizer is installed should be performed to check if there is improvement and how much it is achieved.

4 Differences between the RCP and LCP bands

We have investigated the difference between the spectra obtained with the RCP and LCP channels for the 23 GHz receiver. The power along the band depends on the IF at both polarizations, the cables, connectors and the preprocessor unit just before the FFT backend. Fig. 6 shows a simple layout of these elements from the receivers to the FFT backend.

In order to investigate the influence of each part we have used three configurations which combine the elements in different ways. These configurations do not cover all possible connections, only some basic ones.

- First configuration is what we call ”RCP+CAB1+PP1” for channel 1 and ”LCP+CAB2+PP2” for channel 2. RCP stands for Right Circular Polarization, CAB1 for IF Cable 1, a long

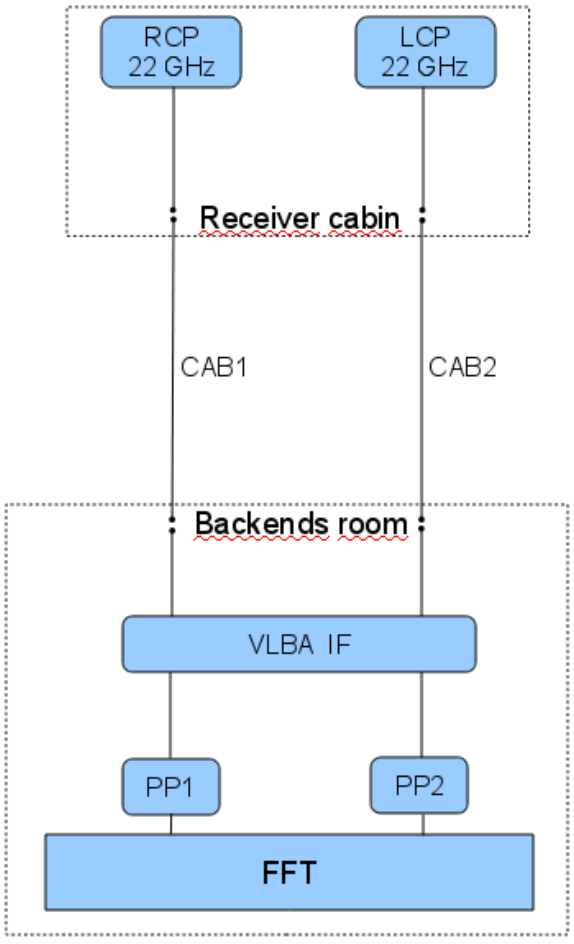

Figure 6: *Schematics of the IF setup for both polarizations of the 23 GHz receiver. Cables 1 and 2 are interrupted at patch panels in the receiver cabin and the backends room. The connections in the patch panel are displayed as dots at the ends of the lines.*

cable (30 m long approximately) connecting the receiver cabin patch panel and the backends patch panel and PP1 stands for Preprocessor unit 1. The other two configurations are derived from this one.

- Second configuration is "LCP+CAB2+PP1" and "RCP+CAB1+PP2". This was done by switching the IF cables at the backends patch panel.
- Third configuration is "LCP+CAB1+PP1' and "RCP+CAB2+PP2". This was achieved by switching IF cables at the receiver cabin patch panel.

Fig. 7 shows 4 panels with the results from some combinations. Fig. 7a shows two curves with the output of the LCP band receiver being detected by preprocessor 1: one goes along cable CAB1 and the other along cable CAB2. There is a very slight difference between both, from which we can conclude that ripples along the band probably do not come from the cables. Fig. 7b shows exactly the same behaviour but with the signal from the RCP channel and preprocessor 2.

Fig. 7c shows two curves: one is the signal from RCP channel along cable 1 entering in preprocessor 1 and the second curve is the same signal entering in preprocessor 2. "High frequency" ripples along the band are different for both cases which probably means they arise from the preprocessor modules: each preprocessor has a different signature.

Fig. 7d shows both polarizations along the same cable and detected with the same preprocessor. Ripples depending on frequency are approximately the same, although there is a power level difference between both channels. The power level difference is not constant along the band.

We conclude that the power decay along the band is due to the length of the IF cables, and most of the ripples and features seen along the band arise in the preprocessor modules. Probably the latter is due to the use of amplifiers.

We have also investigated this behaviour with the 3 mm receiver for which we have a single polarization. Results are shown in Fig. 8

The 3 mm IF results allow to extract the same conclusions as the 22 GHz IF: most of the ripples and gain variations come from the preprocessor. Cables do not introduce any significant gain variation, except a power drop which depends on the frequency. It seems that this continuous power loss also depends on the IF of the receivers. The 22 GHz receiver shows a larger drop of power along the band than the 87 GHz one (see Fig. 9).

5 Studying the band pass with thermal lines

In order to study the variability of the noise and the amplitude of the signal along the band we have tried to calibrate it by observing a narrow thermal line along the IF band. We have observed NH_3 1(1)-1(1), NH_3 2(2)-2(2) and NH_3 3(3)-3(3) towards L1157B1, a source with a strong ammonia emission. The first transition shows hiperfine structure with multiple lines while NH_3 2(2)-2(2) and NH_3 3(3)-3(3) show a single feature. All lines were observed with different local oscillator setups. Some of these setups did not allow to have the three lines simultaneously. In order to get a reasonable SNR we integrated for 20 minutes. Final SNR was 5 for NH_3 3(3)-3(3), 5.5 for NH_3 2(2)-2(2) and 27 for NH_3 1(1)-1(1).

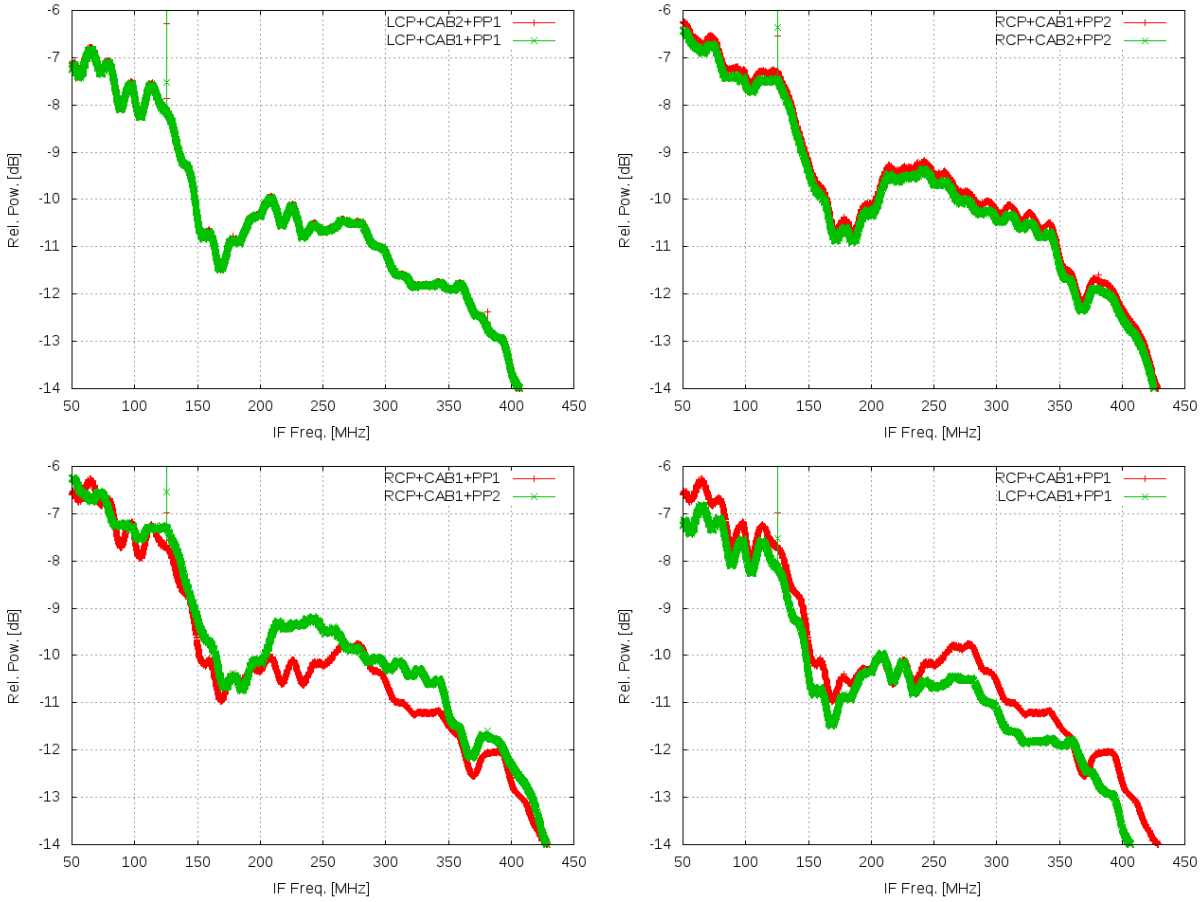

Figure 7: *Power spectrum of the 23 GHz IF at both polarizations with three different configurations. The comparison of the configurations allows to determine which part in the IF chain has a stronger influence on the signal along the frequency band.*

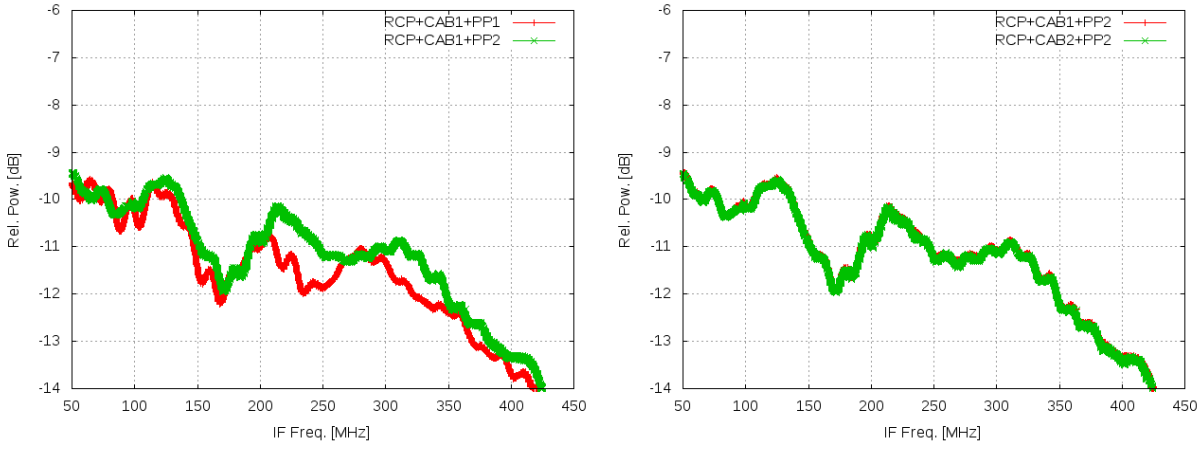

Figure 8: *Power spectrum of the 87 GHz IF with three different configurations. The comparison of the configurations allows to determine the fingerprint of each element in the IF chain up to the backend.*

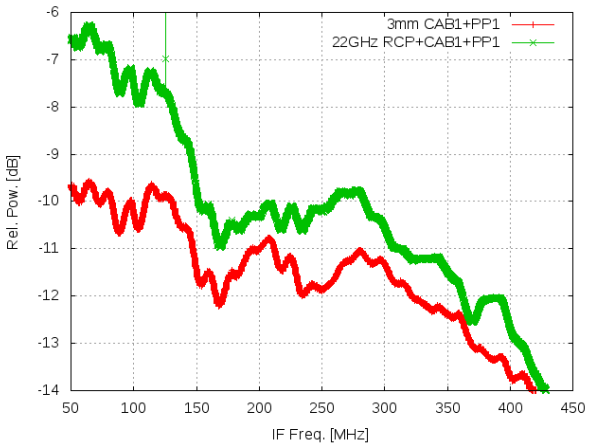

Figure 9: *Power spectrum of the 87 GHz and the 22 GHz IFs with the same cables and preprocessor.*

We used 8 different setups in which the local oscillator frequency was shifted 50 MHz every time. Table 1 summarizes the results.

Sky Freq	NH_3 3(3)-3(3)				NH_3 2(2)-2(2)				NH_3 1(1)-1(1)			
	RCP		LCP		RCP		LCP		RCP		LCP	
	RMS	T_a*	RMS	T_a*	RMS	T_a*	RMS	T_a*	RMS	T_a*	RMS	T_a*
23600					0.013	0.08	0.017	0.12	0.014	0.34	0.020	0.51
23650	0.005	0.05	0.004	0.04	0.014	0.09	0.020	0.17	0.016	0.41	0.020	0.50
23700	0.009	0.13	0.006	0.08	0.020	0.13	0.020	0.11	0.020	0.41	0.03	0.59
23750	0.017	0.16	0.015	0.18	0.020	0.18	0.027	0.15	0.02	0.45	0.025	0.47
23800	0.024	0.19	0.024	0.20	0.028	0.15	0.028	0.19	0.038	0.62	0.033	0.65
23850	0.025	0.31	0.023	0.22	0.049	0.24	0.045	0.22	0.05	0.93	0.047	0.86
23900	0.023	0.23	0.028	0.23	0.05	0.31	0.050	0.28	0.06	1.0	0.06	1.2
23950	0.024	0.21	0.05	0.22	0.07	0.44	0.08	0.42				
24000	0.054	0.46	0.05	0.41								

Table 1: *Intensity and noise RMS for each of the lines using different local oscillators. Only line 3(3)-3(3) is present in all setups.*

As we can see from Table 1, the amplitude calibration along the band is variable and it is the cause for the apparent difference of peak to peak noise (and noise RMS) along the band. It seems clear that this amplitude calibration difference arises from variations in the input power level which depends on the frequency. It also seems clear that the ripples seen after averaging many ON-OFF scans also come from a difference in power level, which is not removed by the substraction between the ON and OFF subscans. In next section we describe the software solution we have implemented to correct for a calibration which depends on the frequency of the IF.

6 Calibrating the band pass

The problems described in previous sections arise because the gain of our amplifying chain depends on the IF frequency and time. If we assume that the gain dependency on time is slow, this dependency can be removed by on-off scans. The faster the switch between both subscans the better. In other telescopes a wobbler swith or a chopper wheel are used to correct for time variations of the gain. For the time being the 40m lacks these systems, and we use spatial on and off subscans 30 seconds long. Shorter integration times are not optimal since much time would be wasted slewing between the source and the reference position. We assume that both the atmosphere and the receiver chain do not change in a time scale of 1 minute. This asumption may be wrong as the frequency increases and if the atmosphere is unstable.

The dependency of the instrumental gain on frequency is not removed by the spatial on-off scheme. The voltage detected for each subscan is as follows:

$$\begin{aligned} V_{on}(f) &= T^{on}_{sys}(t,f)\,G(t,f) + V_0(t,f) \simeq Tsys^{on}(f)\,G(f) + V_0 \\ V_{off}(f) &= T^{off}_{sys}(t,f)\,G(t,f) + V_0(t,f) \simeq Tsys^{off}(f)\,G(f) + V_0 \end{aligned}$$

where $V_{on}(f)$ is the detected voltage towards the source and $V_{off}(f)$ is the voltage towards the reference position. $G(t,f)$ is the gain of the receiver chain and it is a function of frequency and time. T_{sys} is the system temperature. We have assumed that all variables are independent of time during the time scale of an ON-OFF scan and hence we have removed this dependency. Assuming that the reference position is close to the source position, the system temperature difference between both positions is the antenna temperature, $T_a(f)$ which depends on the frequency. We have also assumed that $V_0(t,f)$ (the voltage offset) is independent of frequency and indeed this is an important choice since the usage of an FFT backend can generate artifacts in several frequency channels, see Fig. 10 for an example. In that example V_0 is several orders of magnitude lower than signals from the sky and the average is justified.

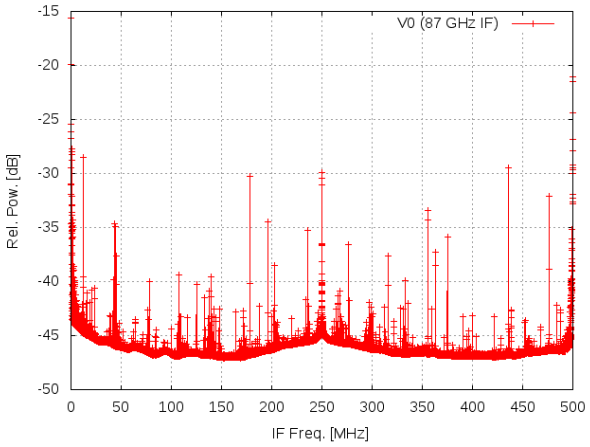

Figure 10: *Power spectrum of the 87 GHz IF when mesuring the zero voltage offset. There are artifacts on some frequency channels. The zero is obtained by connecting to an empty input at the VLBA terminal and attenuating the signal by 20 dB.*

Substracting both voltages we get:

$$V_{on}(f) - V_{off}(f) \simeq Ta(f)\, G(f)$$

In all spectra displayed in previous sections we have considered that the gain was not frequency dependent:

$$G(f) = G_0$$

$G(f)$ can be determined using a calibrated noise diode like for receivers at C band, X band and 22 GHz or hot and cold loads for the 87 GHz receiver.

When using a noise diode:

$$\begin{aligned} V_{on}(f) &= (T_a(f) + T_{rec} + T_{atm})G(f) + V_0 \\ V_{off}(f) &= (T_{rec} + T_{atm})G(f) + V_0 \\ V_{diodeoff}(f) &= (T_d(f) + T_{rec} + T_{atm})G(f) + V_0 \end{aligned}$$

where we have assumed that neither the receiver temperature nor the atmosphere temperature depend on frequency along the IF band (currently, 500 MHz). $V_{diodeoff}(f)$ is the voltage towards the reference position with the noise diode switched on, T_{rec} is the receiver temperature and T_{atm} is the antenna temperature towards the sky and we have assumed that there is no frequency dependence along the detecting band. T_d is the noise diode temperature and depends on the frequency. Calibration is achieved by subsctracting the on and off subscans and dividing by the difference of the signal towards the reference when the noise diode is switched on and off:

$$T_a(f) = \frac{V_{on}(f) - V_{off}(f)}{V_{diodeoff}(f) - V_{off}(f)} T_d(f) \tag{1}$$

The pipeline software used until January 24th 2011 approximated the previous expression by assuming that the noise diode temperature and the voltages with the noise diode off and on were not frequency dependent:

$$T_a^s(f) = \frac{V_{on}(f) - V_{off}(f)}{< V_{diodeoff} > - < V_{off} >} T_d \tag{2}$$

and this lead to the results shown in previous sections. V_{off} and $V_{diodeoff}$ where obtained averaging the values for the whole frequency band. The noise diode temperature is also an average of the ones provided by the lab. The decission to use averages was taken because the noise diode temperature had an apparent random dependency of frequency. We believe that this random behaviour is due to reflections on the cables, rather long, between the noise diode and the directional coupler in the cryostat and to temperature variations in the cabin.

In order to calibrate observations, FITs files generated from the the 40 m radiotelescope contain an HDU which holds, among other values, the voltage from the noise diode on the source and off the source, the voltage on the source and off the source and the zero from the last calibration scan. These values are scalars, and hence obtained by averaging the voltages along the band. Including these voltages as arrays requires non-simple modifications in the pipeline and we have tried to avoid it and find simpler solutions which allow to make a calibration dependent on frequency.

Two solutions are possible:

- It is possible to recover the gain as a function of frequency by multiplying expression 2 by the following factor:

$$K = \frac{< V_{off} >}{V_{off}(f)}$$

Let us see why: if we rewrite,

$$< V_{off}(f) > - < V_{diodeoff}(f) >= T_d \ < G(f) >$$

then expression 2 can be written as:

$$T_a^s(f) = \frac{V_{on}(f) - V_{off}(f)}{< G(f) >}$$

on the other hand:

$$T_a(f) = \frac{V_{on}(f) - V_{off}(f)}{G(f)}$$

then:

$$\begin{aligned} T_a(f) &= T_a^s(f)\frac{< G(f) >}{G(f)} \\ &= T_a^s(f)\frac{< V_{off} > -V_0}{V_{off} - V_0} \end{aligned}$$

This solution requires a very simple implementation in the software without modifying the FITs file structure. The underlying idea is that we use the reference position (the sky) as a calibration source for the band pass and assume that the sky emission and absorption does not depend on frequency for the frequency interval of the IF band.

- The most straightforward solution is to use expression 1, approximating the noise diode temperature by an average value. This solution requires that the software implementation retrieves the voltage from the calibration scan and applies a calibration per frequency channel. From a practical point of view we have implemented this by adding an extra keyword with the number of the last calibration scan which has the same frontend-backend combination. The pipeline reads this scan and retrieves the required voltages as arrays.

Calibration with hot and cold loads requires a calibration per frequency channel and assuming that the temperature of the cold and hot loads is independent of frequency. This is a good approximation if the hot and cold loads acts as black bodies and the band pass is at most 2 GHz wide.

When using a hot cold load:

$$\begin{aligned} V_{on}(f) &= (T_a(f) + T_{rec} + T_{atm})G(f) + V_0 \\ V_{off}(f) &= (T_{rec} + T_{atm})G(f) + V_0 \\ V_{hot}(f) &= (T_h + T_{rec})G(f) + V_0 \\ V_{cold}(f) &= (T_c + T_{rec})G(f) + V_0 \end{aligned}$$

where T_{rec} and T_{atm} are the receiver and atmosphere temperatures respectively and we have approximated them as scalars, T_h and T_c are the hot and cold temperature respectively and are also considered to be independent of frequency. $V_{hot}(f)$ is the voltage measured when observing the hot load and $V_{cold}(f)$ the voltage when observing the cold load. Both are frequency dependent due to the instrumental gain dependency on frequency.

The antenna temperature is:

$$T_a(f) = \frac{V_{on}(f) - V_{off}(f)}{V_{hot}(f) - V_{cold}(f)}(T_h - T_c)$$

From the practical point of view, the calibration per channel of frequency was implemented as described above: the FITs files contains the scan number of the last calibration scan and the pipeline retrieves the voltages for the cold and hot loads to use them in the calibration process.

Fig. 11 shows an ON-OFF averaged spectra with a scalar (frequency independent) and vectorial calibration (frequency dependent) respectively at 87 GHz. The vectorial calibration removes all nasty effects described in this report.

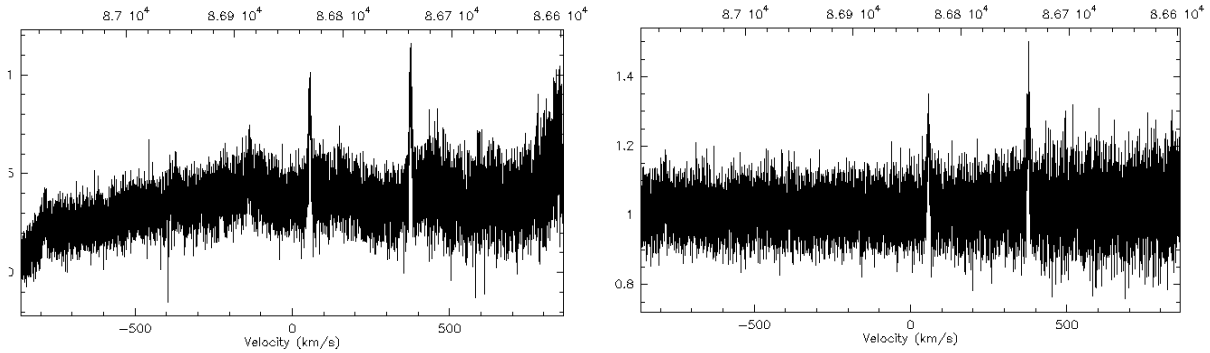

Figure 11: *Left: On-off spectrum at 87 GHz towards W51-E1 with scalar (frequency independent) calibration. Right: The same spectrum with a vectorial (frequency dependent) calibration.*

7 Examples of spectra with the new calibration scheme

Fig. 12 shows an spectrum with an integration time of 1000 minutes towards IRC+10216 at 90 GHz. The spectrum was obtained averaging several ON-OFF scans. No baseline has been removed. The lines are HC_3N (11-10) and SiS 5-4.

Fig. 13 shows the spectrum towards CepheusEmm at 6668 MHz, the Methanol maser line CH_3OH 5(1,5)-6(0,6), for an integration time of 30 seconds. We chose this source since there is no maser line and hence it allows to see the IF spectrum. Fig. 14 shows an example where the maser line is clearly detected (at 60 km/s). Strong interferences are also visible.

Fig. 15 shows the spectrum towards 3C345 at 4998 MHz for an integration time of 30 seconds. No known line is present at this frequency band and, as before, that allows to examine the IF spectrum. The RFI is so strong that renders useless any spectral observation at this frequency interval.

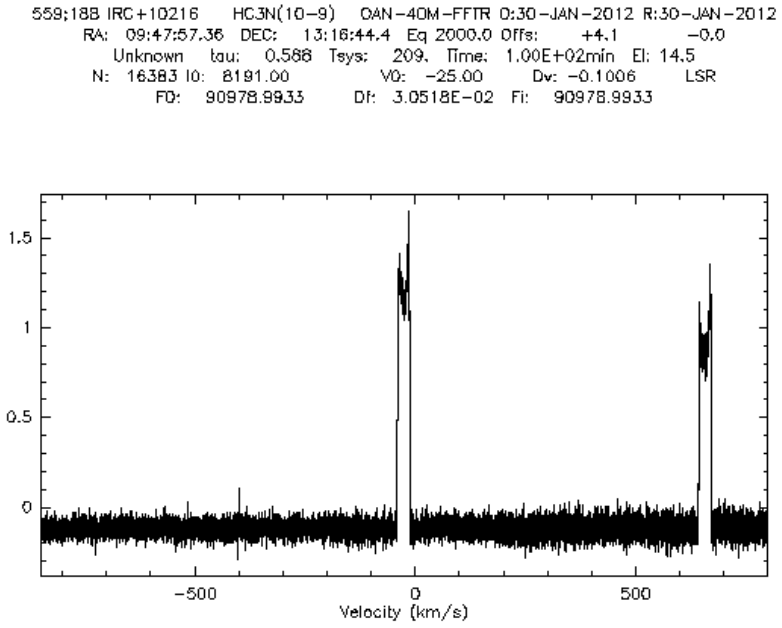

Figure 12: *On-off spectrum at 90 GHz towards IRC+10216 after 100 minutes of integration. No baseline was removed.*

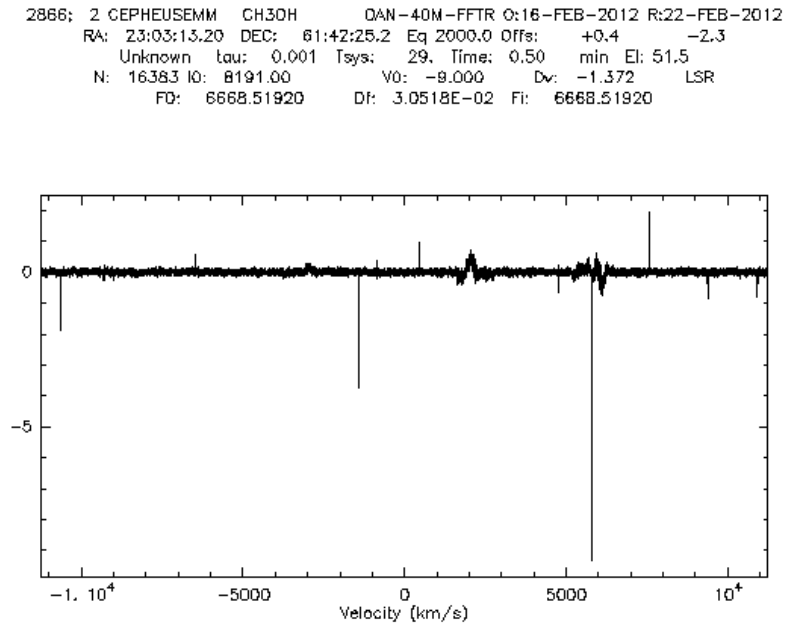

Figure 13: *On-off spectrum at 6668 MHz towards Cepheuse after 30 seconods of integration. No methanol line is detected. No baseline was removed.*

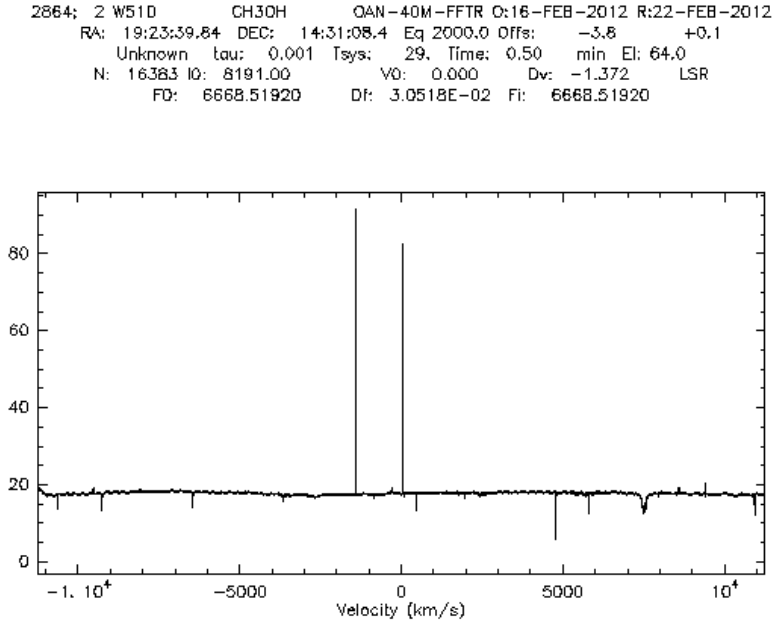

Figure 14: *On-off spectrum at 6668 MHz towards W51D after 30 seconds of integration. CH_3OH 5(1,5)-6(0,6) line at 60 km/s. The narrow line at No baseline was removed.*

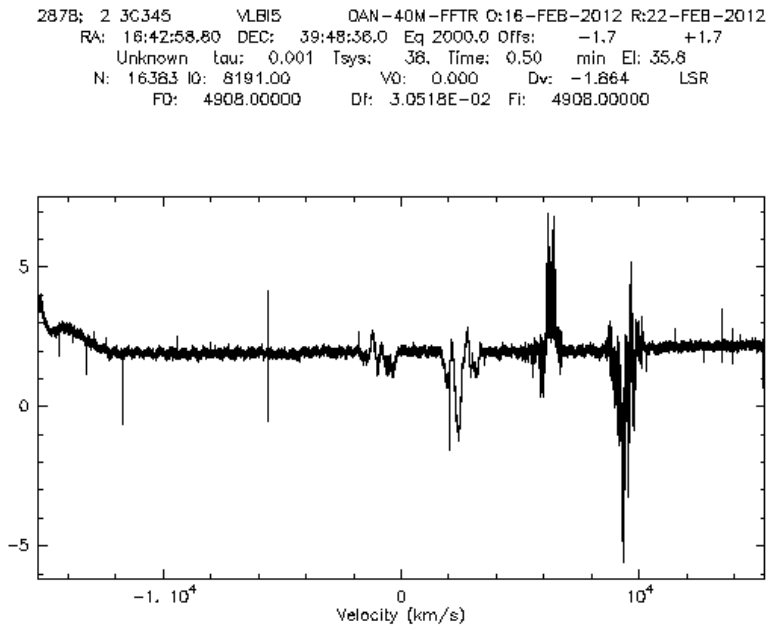

Figure 15: *On-off spectrum at 4990 MHz towards 3C345 after 30 seconds of integration. Strong RFI in the band is seen. No baseline was removed.*

Fig. 16 shows the spectrum towards Cepheus A at 23822 MHz for an integration time of 20 minutes. From left to right the detected lines are: NH_3 3(3)-3(3), NH_3 2(2)-2(2) and NH_3 1(1)-1(1).

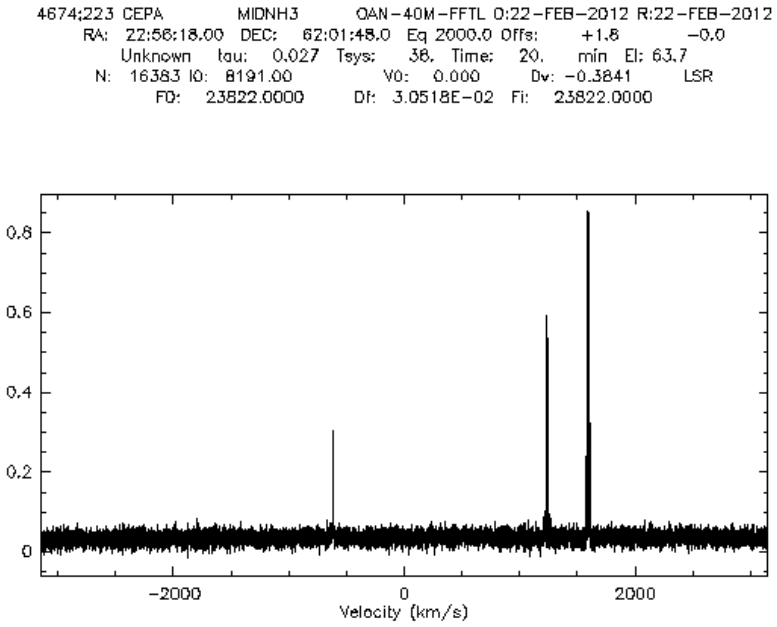

Figure 16: *On-off spectrum at 23822 MHz towards Cepheus A after 20 minutes of integration. NH_3 transitions 3(3)-3(3), 2(2)-2(2) and 1(1)-1(1) are detected. No baseline was removed.*

8 Observed and theoretical expected noise

We have investigated the noise RMS obtained by removing a baseline to spectra after some integration time and compared the results from the RMS computed from the bandwidth of each individual channel (B), the integration time (τ) and the system temperature (T_{sys}) assuming that the receiver has white noise. The radiometric formula used is:

$$\sigma = \frac{T_{sys}}{\sqrt{B\tau}} \tag{3}$$

We find a discrepancy of factor 2-3 for the 87 GHz receiver and 3-4 for the 22 GHz receiver; observed RMS is larger in both cases than the theoretical one obtained using the previous expresion. This difference may arise from non white noise in the receivers. This difference is larger (up to a factor 10) with continuum observations where the total bandwidth is 500 MHz (Gallego 2008).

For example the spectrum displayed in Fig. 12 has a frequency resolution of 30 KHz per channel, the integration time is 100 minutes and the system temperature 209 K. The expected

RMS is 0.011 K, where we have assumed that $\tau = 12000$ s since it should contain the ON plus the OFF integration times. The observed RMS from a base line fit is 0.0397 K. The difference between both is 2.5.

References

[Gallego 2008] J.D. Gallego. Preliminary measurements of the gain fluctuation of the 22 GHz receiver of the 40m Yebes antenna. IT OAN 2008-17.